

Ab initio configuration interaction study of the low-lying $1\Sigma^+$ electronic states of LiCl

P. F. Weck^{a)}

Department of Physics and Astronomy and Center for Simulational Physics, The University of Georgia, Athens, Georgia 30602-2451

K. Kirby^{b)}

Institute for Theoretical Atomic, Molecular and Optical Physics, Harvard-Smithsonian Center for Astrophysics, Cambridge, Massachusetts 02138

P. C. Stancil^{c)}

Department of Physics and Astronomy and Center for Simulational Physics, The University of Georgia, Athens, Georgia 30602-2451

(Received 6 November 2003; accepted 3 December 2003)

Ab initio configuration interaction calculations have been performed for the $X^1\Sigma^+$ and $B^1\Sigma^+$ electronic states of LiCl. Potential energy curves, dipole moment functions, and dipole transition moments have been computed for internuclear distances between $R=2.5a_0$ and $50a_0$. Single- and double-excitation configuration interaction wave functions were constructed using molecular orbitals obtained from a two-state averaged multiconfiguration self-consistent-field calculation. This procedure yielded an accurate energy splitting between the covalent and ionic separated-atom limits. The calculated avoided crossing of the X and B state curves occurs at $R=16.2a_0$, in close agreement with previous calculations using a semiempirical covalent–ionic resonance model. $X^1\Sigma^+$ state spectroscopic constants are in excellent agreement with experimental values. © 2004 American Institute of Physics. [DOI: 10.1063/1.1643715]

I. INTRODUCTION

Since the earliest days of quantum chemistry, alkali metal halides have played a central role in the understanding of the ionic bond¹ as well as in the development of the Landau–Zener method^{2,3} for treating curve crossings. Recently, alkali metal halides have also been the subject of a number of theoretical and experimental studies of quantum control of chemical reactions,^{4–7} showing the crucial importance of accurate potential energy curves for quantitative comparison with experiments.

Among the alkali halides, lithium chloride has received particular experimental attention.^{8–14} On the theoretical front, investigations have focused mainly on the electronic structure and properties of the $X^1\Sigma^+$ potential in the equilibrium region and on the crossing region of the $X^1\Sigma^+$ and $B^1\Sigma^+$ states.^{15–21} However, no *ab initio* potential energy curves and dipole moments covering the complete range of internuclear separations have been reported, to our knowledge, for these two low-lying electronic states of LiCl. In fact, the only complete potential curves available were calculated using a covalent–ionic resonance model combined with a semiempirical valence-bond method.^{15,17} Although this conceptually simple method has been shown to be valuable in describing the intermediate and large internuclear separation range, its lack of valence-bond structures corresponding to Rydberg states is expected to overestimate the

repulsive character of the $B^1\Sigma^+$ state at short range.²² In particular, this may lead to considerable errors in any photodissociation rate calculation of LiCl, which is of interest for astrophysical considerations.

In contrast to the dearth of *ab initio* treatments of LiCl, the LiF molecule and the ionic–covalent interaction of its $X^1\Sigma^+$ and $B^1\Sigma^+$ states have been the object of numerous quantum chemical studies.^{19,23–25} As was discovered in these *ab initio* treatments, the X and B states are best described by some form of state-averaged multiconfiguration self-consistent-field (MCSCF/SA) optimization to obtain orbitals appropriate for the description of both the ionic and the covalent characters of the states.

In this work, we present multireference single- and double-excitation configuration interaction (MRSDCI) results for the $X^1\Sigma^+$ and $B^1\Sigma^+$ electronic states of LiCl. Adiabatic potential energy curves and dipole moment functions have been evaluated for internuclear separations ranging from $R=2.5a_0$ to $50.0a_0$. A two-state weighted average procedure was adopted to calculate the MCSCF molecular orbitals, in order to reproduce the experimental energy splitting between the separated-atom limits of the X and B states in our final MRSDCI calculations. We compare our results for the $X^1\Sigma^+$ potential with the fit of Ogilvie,¹⁶ in the equilibrium region, obtained by direct spectral inversion of vibration–rotation transitions. Comparison is also made with previous theoretical results for the $X^1\Sigma^+$ and $B^1\Sigma^+$ states calculated with the semiempirical valence-bond method of Zeiri and Balint-Kurti.^{15,17} Vibrationally averaged dipole mo-

^{a)}Electronic mail: weck@physast.uga.edu

^{b)}Electronic mail: kirby@cfa.harvard.edu

^{c)}Electronic mail: stancil@physast.uga.edu

TABLE I. Slater-type function basis set for LiCl.

Li		Cl	
nl	$\zeta(a_0^{-1})$	nl	$\zeta(a_0^{-1})$
1s	4.6351	1s	19.4328
1s	2.473	1s	14.328 44
2s	1.033	2s	11.441 09
2s	0.8237	2s	6.939 64
2s	0.51	2p	11.136 31
2p	3.9004	2p	6.046 72
2p	2.1109	3s	5.30
2p	1.0758	3s	4.241 41
2p	0.7539	3s	2.637 53
2p	0.51	3s	1.728 65
3s	2.6811	3p	4.0
3d	1.4974	3p	3.305 56
3d	0.9866	3p	1.998 19
4f	1.7748	3p	1.295
		3d	3.306
		3d	1.998
		3d	1.295
		4s	1.1
		4p	0.4
		4d	1.45
		4f	2.57
		4f	1.665

ments for the $X^1\Sigma^+$ state are also reported. Atomic units are used throughout unless otherwise stated.

II. CALCULATIONS

The two lowest-lying separated atom limits for LiCl are the ground state atoms, $\text{Li}(^2S_g) + \text{Cl}(^2P_u)$, and the ion pair, $\text{Li}^+(^1S_g) + \text{Cl}^-(^1S_g)$. In this work we neglected the spin-orbit splitting of the ground state chlorine levels, $\text{Cl}(^2P_{1/2})$ and $\text{Cl}(^2P_{3/2})$. The asymptotic energy separation of the covalent and ionic limits is estimated to be 1.74 eV, which was calculated by taking the ionization potential of Li to be 5.392 eV (Ref. 26) and by adjusting the Cl electron affinity of 3.617 eV (Ref. 27) to account for the fine-structure averaged electron affinity of Cl which gave a value of 3.653 eV. Each of these asymptotic limits gives rise to a molecular state of $1\Sigma^+$ symmetry. At very large distances, as the internuclear separation, R , decreases, the upper state is governed by the Coulomb attraction and the lower state energy remains relatively flat. In the vicinity of $R=15-16.5a_0$, the two states experience an avoided crossing and the lower state becomes dominated by ionic character, giving rise to considerable binding and the upper state takes on covalent character, showing no binding at short range. Electronic energies and wave functions were calculated for these states as a function of internuclear separation using the configuration interaction (CI) method.

A basis set of Slater-type functions centered on the atomic nuclei was used to construct an orthonormal set of molecular orbitals. The basis set, given in Table I, included 36σ , 21π , 9δ , and 3ϕ functions. For chlorine, the $(9s/7p/4d/2f)$ basis set from the HCl^+ study of Pradhan, Kirby, and Dalgarno²⁸ was used. The basis set for lithium was adopted from the calculations of LiH^+ of Dalgarno,

Kirby, and Stancil.²⁹ All calculations were performed using the ALCHEMY II *ab initio* quantum chemistry codes developed by Mc Lean *et al.*³⁰

At each internuclear separation, molecular orbitals used to construct the electronic wave functions were obtained from a state-averaged multiconfiguration self-consistent-field (MCSCF/SA) calculation involving the the complete active space of the 6σ , 7σ , 8σ , and 2π orbitals, with six electrons distributed among them. The $1\sigma-5\sigma$ and 1π orbitals were taken to be frozen, SCF-determined, core orbitals. A number of different weights were explored in the state-averaged MCSCF, and there was considerable sensitivity exhibited in the convergence of the MCSCF calculation to the weights of the states used. It was found that a 0.35/0.65 weighting of the ground and first excited states, respectively, resulted in orbitals which, when used in the single- and double-excitation CI wave function reproduced the experimental splitting of the asymptotic limits to within 0.001 eV at $R=10\,000a_0$. It was extremely important to the calculation of the two states in the avoided crossing region that this asymptotic splitting was as accurate as possible.

Multireference configuration interaction wave functions (MRSDCI) were constructed by including all single and double excitations from the same reference space which was used for the MCSCF calculations. There were a total of 134, 163 configuration state functions for the MRSDCI calculations, and 76 configuration state functions in the reference space.

Some convergence difficulties in the MCSCF/SA calculation in the region between $R=10a_0$ and $R=15a_0$ were experienced. This appeared to result from the two lowest roots oscillating between two local minima. The weighted trace of the energies of the X and B states was identical for the two local minima in this region. By slightly changing the state-averaged weights in this region, by just a few percent to a maximum 0.46/0.54 mixture at $R=12a_0$, for instance, convergence was obtained. The resulting MRSDCI potential curves in this region showed no unevenness or oscillations, so the resulting description of the wave function did not appear to be compromised.

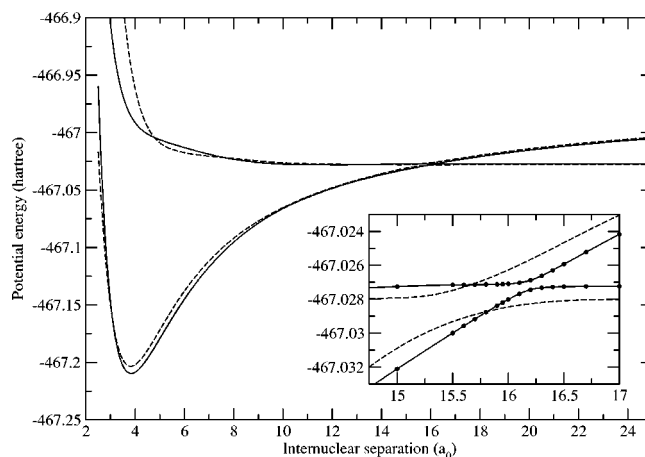
III. RESULTS AND DISCUSSION

A. Potential energy curves

In Table II we present the adiabatic MRSDCI energies at 69 internuclear separations in the range $2.50 \leq R \leq 50.00a_0$ for the $X^1\Sigma^+$ and $B^1\Sigma^+$ electronic states. Figure 1 shows the potential energy curves obtained by cubic spline interpolation from the calculated energies of Table II. For the $B^1\Sigma^+$ state, the differences arising between our MRSDCI calculations and the semiempirical calculations of Cooper, Bienstock, and Dalgarno¹⁷ may be attributed to several approximations inherent in the model of Zeiri and Balint-Kurti.¹⁵ At short range, the lack of valence-bond structures corresponding to Rydberg states translates into a significant overestimation of the repulsive character of the $B^1\Sigma^+$ potential.²² Moreover, in the internuclear separation range $4.8 \leq R \leq 7.6a_0$, the $B^1\Sigma^+$ valence-bond potential curve lies lower than the MRSDCI results. This difference may be explained

TABLE II. MRSDCI potential curves of the X and B states of LiCl (energies in Hartrees).

$R(a_0)$	$X^1\Sigma^+$	$B^1\Sigma^+$
2.50	-466.959 707	-466.741 486
2.60	-467.014 713	-466.787 833
2.70	-467.059 443	-466.826 234
2.80	-467.095 542	-466.857 963
2.90	-467.124 438	-466.884 122
3.00	-467.147 349	-466.905 656
3.10	-467.165 308	-466.923 364
3.20	-467.179 181	-466.937 917
3.30	-467.189 690	-466.949 876
3.40	-467.197 436	-466.959 707
3.50	-467.202 918	-466.967 796
3.60	-467.206 549	-466.974 459
3.70	-467.208 670	-466.979 959
3.80	-467.209 561	-466.984 510
3.81	-467.209 592	-466.984 920
3.82	-467.209 613	-466.985 322
3.83	-467.209 625	-466.985 717
3.84	-467.209 627	-466.986 105
3.85	-467.209 620	-466.986 486
3.90	-467.209 456	-466.988 288
4.00	-467.208 546	-466.991 436
4.20	-467.204 913	-466.996 299
4.50	-467.196 571	-467.001 212
4.80	-467.186 476	-467.004 520
5.00	-467.179 363	-467.006 251
5.50	-467.161 609	-467.009 841
6.00	-467.145 020	-467.013 045
6.50	-467.130 128	-467.016 068
7.00	-467.116 991	-467.018 835
7.50	-467.105 478	-467.021 240
8.00	-467.095 402	-467.023 226
8.50	-467.086 577	-467.024 797
9.00	-467.078 835	-467.025 991
9.50	-467.072 035	-467.026 863
10.00	-467.066 056	-467.027 465
10.50	-467.061 004	-467.027 739
11.00	-467.056 435	-467.027 906
11.50	-467.052 323	-467.027 977
12.00	-467.048 556	-467.028 022
12.50	-467.045 128	-467.028 028
13.00	-467.042 054	-467.027 937
13.50	-467.039 254	-467.027 804
14.00	-467.036 672	-467.027 653
14.50	-467.034 329	-467.027 423
15.00	-467.032 109	-467.027 252
15.50	-467.029 989	-467.027 151
15.60	-467.029 575	-467.027 147
15.70	-467.029 167	-467.027 142
15.80	-467.028 767	-467.027 133
15.90	-467.028 379	-467.027 119
15.95	-467.028 191	-467.027 108
16.00	-467.028 009	-467.027 092
16.10	-467.027 679	-467.027 031
16.20	-467.027 440	-467.026 883
16.30	-467.027 325	-467.026 616
16.40	-467.027 278	-467.026 285
16.50	-467.027 256	-467.025 934
16.70	-467.027 238	-467.025 221
17.00	-467.027 230	-467.024 165
17.50	-467.027 230	-467.022 474
18.00	-467.027 232	-467.020 874
19.00	-467.027 239	-467.017 926
20.00	-467.027 246	-467.015 274
22.00	-467.027 257	-467.010 700
25.00	-467.027 265	-467.005 212
28.00	-467.027 270	-467.000 909
30.00	-467.027 272	-466.998 521
35.00	-467.027 275	-466.993 751
50.00	-467.027 277	-466.985 171

FIG. 1. Adiabatic potential energy curves of the $X^1\Sigma^+$ and $B^1\Sigma^+$ states of LiCl. Solid curve, two-state averaged MRSDCI calculation; dashed curve, semiempirical valence-bond calculations of Cooper *et al.* (Ref. 17).

by the approximate treatment of the effective core–core interaction in their valence-bond model.¹⁵ Indeed, the effective core–core interaction, in which each effective core absorbed all the electrons of the doubly occupied orbitals, was defined by requiring that the calculated $X^1\Sigma^+$ potential curve agrees with the Rittner potential of Brumer and Karplus.³¹ While keeping unchanged the electron–electron repulsion and one-electron Hamiltonian matrix elements between the valence-bond structures, this adjustment has the consequence of decreasing the effective core–core interaction term. This alteration is particularly visible as the internuclear separation decreases and the core–core repulsion becomes stronger. For $R \leq 4.8a_0$, this effect is merely masked by the strongly repulsive wall due to the absence of Rydberg character as discussed above; a more accurate description of the core–core interaction would result in a potential curve with even more repulsive behavior. The discrepancies shown in Fig. 1 can also be ascribed, to some extent, to the approximate determination of the mixing coefficients of the covalent and ionic valence-bond structures composing the electronic wave function of Σ^+ symmetry which were obtained by use of the two-electron valence-bond model of Zeiri and Shapiro.³²

At larger internuclear separations, an avoided crossing arises between the ionic $X^1\Sigma^+$ and the covalent $B^1\Sigma^+$ states, thereby leading to the formation of a small minimum in the adiabatic potential curve of the $B^1\Sigma^+$ state. The MRSDCI calculations, for which the Cl fine structure was not resolved, yielded a distance of $R_c = 16.2a_0$ for the avoided crossing, in excellent agreement with the fine-structure averaged value $R_c = 16.05a_0$ obtained from the crossing distance values $R_c(^2P_{3/2}) = 15.71a_0$ and $R_c(^2P_{1/2}) = 16.73a_0$ calculated by Cooper *et al.*¹⁷ for the $\text{Li}(^2S_{1/2}) + \text{Cl}(^2P_{3/2})$ and $\text{Li}(^2S_{1/2}) + \text{Cl}(^2P_{1/2})$ curves, respectively. The MRSDCI crossing point value is slightly larger than the $R_c = 15.7a_0$ distance obtained by Zeiri and Balint-Kurti.¹⁵ The inclusion of spin–orbit interaction in our calculations would be expected to lower the dissociation asymptote of the $X^1\Sigma^+$ state somewhat and shift the avoided crossing distance to smaller internuclear separations.³³ However, the spin–orbit splitting in atomic chlorine,

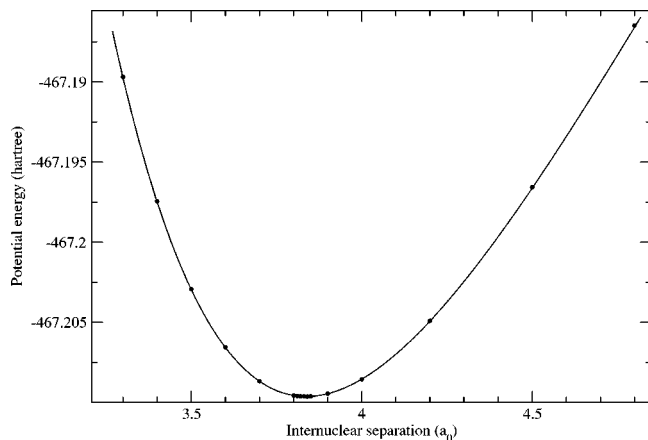


FIG. 2. Adiabatic potential energy curves of the $X^1\Sigma^+$ state of LiCl. Circles, two-state averaged MRSDCI calculation; solid curve, experimentally derived fit of Ogilvie (Ref. 16).

$\Delta E_{so} = 4.0203 \times 10^{-3}$ a.u.,³⁴ is relatively insignificant compared to the electron affinity and the corrections to the crossing distance of this study are expected to be much less than one Bohr. Thus, the values $R_c = 15.1a_0$ and $R_c = 14.74a_0$ predicted by Sousa *et al.*¹⁹ at the MS-CASPT2 and CASPT2 levels of theory, respectively, most certainly underestimate the crossing point distance due to the lack of dynamical correlation. As depicted in the inset of Fig. 1, the energy separation between the X and B states at the avoided crossing distance is $\Delta E_c = 5.6 \times 10^{-4}$ a.u. for the MRSDCI calculations, smaller by two orders of magnitude than the $\Delta E_c = 2.3 \times 10^{-2}$ a.u. value found by cubic spline interpolation of the calculated energies of Cooper *et al.*¹⁷ Beyond the avoided crossing region, the adiabatic representation of the $B^1\Sigma^+$ state tends to behave as $-1/R$, with dipole polarization corrections proportional to $-1/R^4$.

The interpolated MRSDCI results shown in Fig. 1 yielded an energy minimum of -467.209627 a.u. at $R_e = 3.832a_0$ for the $X^1\Sigma^+$ state, lower than the -467.20339 a.u. value at $R_e = 3.818a_0$ obtained by cubic spline interpolation from the data of Cooper *et al.*¹⁷ In Fig. 2, the energy points from Table II are shown along with the fit to the $X^1\Sigma^+$ potential curve by Ogilvie,¹⁶ for internuclear separations ranging between $3.25a_0$ and $4.80a_0$. For the sake of comparison, a shift in energy of -467.209627 a.u. was applied to the Ogilvie fit, in addition to a shift of $+0.0138a_0$ from the original equilibrium distance of the fit, $R_e = 3.8185a_0$. The fit to the effective potential energy proposed by Ogilvie¹⁶ consisted of a sum of five radial functions accounting empirically for vibrational adiabatic and nonadiabatic effects. The coefficients of this expansion were determined by direct spectral inversion from the frequencies of 2577 known transitions in the infrared and microwave spectral regions for the isotopic variants $^6\text{Li}^{35}\text{Cl}$, $^6\text{Li}^{37}\text{Cl}$, $^7\text{Li}^{35}\text{Cl}$, and $^7\text{Li}^{37}\text{Cl}$. The normalized standard deviation of the fit was 0.993 over the complete range of validity of the radial functions of LiCl, i.e., over the interval of internuclear separations $3.25 \leq R \leq 4.80a_0$. The excellent agreement of our computed energy points with this experimentally derived fit suggests that the normalized standard deviation of our

results for the $X^1\Sigma^+$ potential energy curve is essentially unity in the equilibrium region.

B. Spectroscopic constants

In order to determine the spectroscopic constants of the $X^1\Sigma^+$ potential curve, the vibrational wave functions, $\chi_v(R)$, and energy eigenvalues, $G(v)$, have been calculated by solving with standard Numerov techniques³⁵ the radial nuclear Schrödinger equation,

$$\left[-\frac{1}{2\mu} \frac{d^2}{dR^2} + E_{el}(R) + \frac{J(J+1)}{2\mu R^2} - G(v) \right] \chi_v(R) = 0, \quad (1)$$

where μ is the reduced mass of the system, J is the rotational quantum number corresponding to the angular momentum of nuclear rotation, neglecting the nuclear spin, and $E_{el}(R)$ is the electronic potential energy. The reduced mass adopted for $^7\text{Li}^{35}\text{Cl}$ was 5.8435744 u (Ref. 36) = 10651.3431 a.u.¹¹ Calculations were performed on a grid with stepsize $1 \times 10^{-3}a_0$ for the integration, over a range of internuclear distances from $R = 2.5a_0$ to $200.0a_0$. This outer limit value of the integration range was chosen intentionally large in such a way to obtain a correct energy difference, $D_e = G_{\max}(v)$, between the last discrete vibrational eigenvalue in the vicinity of the dissociation limit and the energy minimum, -467.209627 a.u., obtained at $R_e = 3.832a_0$ from the interpolated $X^1\Sigma^+$ data of Table II. Additional energy points were calculated between $R = 50.0a_0$ and $200.0a_0$ to ensure an accurate description of the long range interaction.

The calculations yielded $D_e = G(207) = 5.03$ eV = 0.1850 a.u. and a zero-point energy $G(0) = 321.00$ $\text{cm}^{-1} = 1.463 \times 10^{-3}$ a.u. As a consequence, the dissociation energy is predicted to be $D_0 = D_e - G(0) = 4.99$ eV = 0.1835 a.u., slightly larger than the thermochemical value, $D_0 = 4.85$ eV, of Brewer and Brackett³⁷ or the flame photometry measurement, $D_0 = 4.79$ eV, of Bulewicz, Phillips, and Sugden.³⁸ As mentioned previously, the introduction of the spin-orbit interaction in our calculations would lower the dissociation asymptote of the $X^1\Sigma^+$ state, thereby bringing the theoretical dissociation energy into closer agreement with the experimental estimates.

The vibrational constants ω_e , $\omega_e x_e$, and $\omega_e y_e$ from the truncated expansion of the energy eigenvalues, $G(v)$, of the anharmonic oscillator,³⁹

$$G(v) = \omega_e \left(v + \frac{1}{2}\right) - \omega_e x_e \left(v + \frac{1}{2}\right)^2 + \omega_e y_e \left(v + \frac{1}{2}\right)^3, \quad (2)$$

were derived from the following identities:

$$\begin{aligned} \omega_e y_e &= \frac{1}{6} (\Delta G_{5/2} - 2\Delta G_{3/2} + \Delta G_{1/2}), \\ \omega_e x_e &= -\frac{1}{2} (\Delta G_{3/2} - \Delta G_{1/2} - 9\omega_e y_e), \\ \omega_e &= \Delta G_{1/2} + 2\omega_e x_e - \frac{13}{4}\omega_e y_e, \end{aligned} \quad (3)$$

with the computed first differences, $\Delta G_{v+1/2} = G(v+1) - G(v)$, given in Table III, along with the values obtained by solving Eq. (1) using the $X^1\Sigma^+$ potential energy fit of Ogilvie.¹⁶ Our calculated values $\omega_e = 644.09$ cm^{-1} , $\omega_e x_e = 4.44$ cm^{-1} , and $\omega_e y_e = 0.02$ cm^{-1} , are in very good agreement with the accurate Dunham constants Y_{10}

TABLE III. Binding energy and $\Delta G_{v+1/2}$ values of the low-lying vibrational levels of the $X^1\Sigma^+$ state (energies in cm^{-1}).

v	BE ^{a,b}	$\Delta G_{v+1/2}$		
		Theory ^b	Ogilvie ^c	Expt. ^d
0	40 281.51	635.28	634.06	634.076
1	39 646.23	626.57	625.29	625.313
2	39 019.67	617.97	616.66	616.675
3	38 401.70	609.52	608.16	608.162
4	37 792.17	601.19	599.81	599.773
5	37 190.98	592.94	591.65	591.510
6	36 598.04	584.82	583.72	583.371
7	36 013.22	576.83	576.03	575.357
8	35 436.39	568.95	568.58	567.468
9	34 867.44	561.16	561.31	559.704
10	34 306.29	553.47	554.18	552.065

^aBinding energies are given for rotationless vibrational levels.

^bThis work.

^cCalculated with the spectral inversion fit of Ref. 16.

^dDerived from the experimental Y_{10} , Y_{20} , and Y_{30} of Ref. 14.

$= 642.958\,13\text{ cm}^{-1}$, $-Y_{20}=4.475\,085\text{ cm}^{-1}$, and $Y_{30}=0.020\,8072\text{ cm}^{-1}$, respectively, derived from experiment by Thompson *et al.*¹⁴ for $^7\text{Li}^{35}\text{Cl}$. The frequency of the first band, $\nu(1-0)=\Delta G_{1/2}=635.28\text{ cm}^{-1}$, almost reproduces the value of 634.076 cm^{-1} , obtained using the Dunham terms given above. As could be expected from Fig. 2, the agreement between the $\Delta G_{v+1/2}$ results evaluated with the MRSDCI potential curve and the fit of Ogilvie¹⁶ is also very good, with differences in energy less than 1.4 cm^{-1} up to $v=10$. Our theoretical $\Delta G_{v+1/2}$ values are in close agreement with the experimentally derived values as v increases, thus reflecting the accuracy of our anharmonic parameters $\omega_e x_e$ and $\omega_e y_e$ over the intermediate separation range. For $v \geq 9$, our $\Delta G_{v+1/2}$ results are in better agreement with experiment than the values computed using the Ogilvie fit, since the latter was constructed by spectral inversion from transitions with a maximum vibrational quantum number $v=8$.¹⁶ The quartic energy term $\omega_e z_e(v+1/2)^4$, neglected in Eq. (2), is expected to have negligible contributions to the discrepancies observed in Table III due to the small value of $Y_{40}=-6.243 \times 10^{-5}\text{ cm}^{-1}$, determined by Thompson *et al.*¹⁴

C. Dipole moments and transition moment

The electric dipole transition moment between two electronic states i and f can be expressed as $D(R)=\langle\psi_f|\mathbf{M}|\psi_i\rangle$, where $\mathbf{M}=-\sum_j\mathbf{r}_j$, in atomic units, is the electric dipole moment operator of the system of N electrons, with position vectors \mathbf{r}_j , and where the integration is to be taken over the whole configuration space of the $3N$ coordinates. For $\Sigma-\Sigma$ electronic transitions, \mathbf{M} reduces to its component along the z axis joining the nuclei, $M_z=-\sum_j z_j$. In the same way, the electric dipole moment for an electronic state is given by the matrix element of the operator

$$\boldsymbol{\mu}=\sum_i \mathbf{r}_i-\sum_l Z_l \mathbf{R}_l, \quad (4)$$

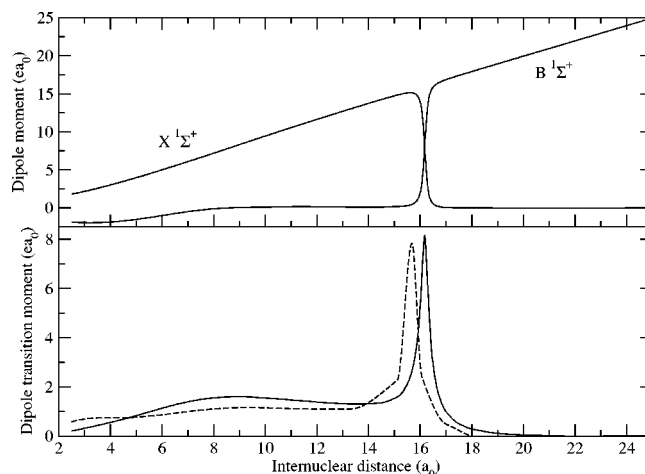
where Z_l are the nuclear charges and \mathbf{R}_l are the position vectors of the nuclei from the center of reference of the operator.

Adiabatic dipole moments for the $X^1\Sigma^+$ and $B^1\Sigma^+$ states are listed in Table IV, together with the $B\leftarrow X$ dipole transition moment values, for internuclear distances between $2.5a_0$ and $50.0a_0$. The curves obtained by cubic spline interpolation from the data of Table IV are shown in Fig. 3, along with the previous results of Zeiri and Balint-Kurti.¹⁵ The strong ionic imprint is illustrated by the linear variation of the X and B adiabatic dipole moments [$D(R)=R$, in atomic units] before and beyond the avoided crossing distance, respectively. At $R_c=16.2a_0$, the dipole moment functions undergo a rapid changeover, signature of the exchange of the ionic and covalent characters between the two electronic states. This discontinuous character is exhibited as well in the $B\leftarrow X$ dipole transition moment with the presence of a sharp peak at this internuclear separation. The calculations of Zeiri and Balint-Kurti¹⁵ predicted a peak of comparable width and intensity and centered at $R_c=15.7a_0$.

For transitions within the $X^1\Sigma^+$ state, the vibrational matrix elements of the electric dipole moment were defined as $\langle v',J'=1|D(R)|v'',J''=0\rangle$, corresponding to $R(0)$ rotational transitions from vibrational levels v'' to vibrational levels v' . The diagonal matrix elements, for which $v'=v''$, are the v -dependent dipole moments, $\mu(v)$. For $^6\text{Li}^{35}\text{Cl}$, our calculations with a reduced mass of $5.132\,2968\text{ u}=9354.866\text{ a.u.}$ yielded for the $X^1\Sigma^+$ state $\mu(0)=7.32\text{ D}$, $\mu(1)=7.41\text{ D}$, and $\mu(2)=7.50\text{ D}$, systematically larger by 0.2 D than the measured values, $\mu(0)=7.1289\text{ D}$, $\mu(1)=7.2168\text{ D}$, and $\mu(2)=7.3059\text{ D}$, obtained by Hebert *et al.*⁴⁰ using the molecular beam electric resonance method. Vibrational matrix elements for the $X^1\Sigma^+$ electric dipole moment of $^7\text{Li}^{35}\text{Cl}$ are reported in Table V for $\mu(v)$ and for the fundamental ($\Delta v=v'-v''=1$) to the second overtone ($\Delta v=3$) transitions. Since the overlap of the initial and final rovibrational wave functions is unity for $\mu(v)$, this diagonal term varies linearly with v for vibrational levels lying far

TABLE IV. Adiabatic X and B dipole moments and dipole transition moment (in atomic units, $e a_0$).

$R(a_0)$	$X^1\Sigma^+$	$B^1\Sigma^+$	$\langle B^1\Sigma^+ M_z X^1\Sigma^+ \rangle$
2.50	1.8203	-1.8674	0.2108
2.60	1.8810	-1.8903	0.2298
2.70	1.9466	-1.9088	0.2509
2.80	2.0163	-1.9234	0.2730
2.90	2.0891	-1.9345	0.2955
3.00	2.1647	-1.9423	0.3182
3.10	2.2424	-1.9469	0.3409
3.20	2.3221	-1.9485	0.3637
3.30	2.4035	-1.9470	0.3866
3.40	2.4864	-1.9426	0.4097
3.50	2.5707	-1.9353	0.4330
3.60	2.6563	-1.9251	0.4566
3.70	2.7431	-1.9121	0.4806
3.80	2.8311	-1.8964	0.5050
3.85	2.8755	-1.8875	0.5174
3.90	2.9202	-1.8779	0.5299
4.00	3.0103	-1.8569	0.5552
4.20	3.1938	-1.8073	0.6071
4.50	3.4763	-1.7150	0.6883
5.00	3.9654	-1.5188	0.8315
5.50	4.4741	-1.2798	0.9816
6.00	4.9985	-1.0144	1.1320
6.50	5.5343	-0.7456	1.2729
7.00	6.0783	-0.4982	1.3939
7.50	6.6292	-0.2912	1.4882
8.00	7.1859	-0.1324	1.5529
8.50	7.7473	-0.0202	1.5889
9.00	8.3117	0.0520	1.5983
9.50	8.8770	0.0923	1.5837
10.00	9.4415	0.1084	1.5473
10.50	9.9956	0.1343	1.5115
11.00	10.5462	0.1434	1.4678
11.50	11.0901	0.1476	1.4277
12.00	11.6303	0.1402	1.3842
12.50	12.1615	0.1379	1.3618
13.00	12.6941	0.1224	1.3173
13.50	13.2182	0.1146	1.2982
14.00	13.7328	0.1150	1.3173
14.50	14.2425	0.1170	1.3535
15.00	14.7224	0.1491	1.5319
15.25	14.9425	0.1843	1.7034
15.50	15.0960	0.2866	2.1115
15.60	15.1224	0.3623	2.3678
15.70	15.1047	0.4820	2.7211
15.80	15.0014	0.6871	3.2294
15.90	14.7059	1.0844	4.0083
15.95	14.4038	1.4375	4.5633
16.00	13.9022	1.9899	5.2708
16.10	11.6140	4.3799	7.1402
16.20	6.6566	9.4388	7.9337
16.30	2.6038	13.5931	5.9588
16.40	1.0800	15.2185	4.0679
16.50	0.5291	15.8708	2.9169
16.70	0.1780	16.4245	1.7422
17.00	0.0518	16.8545	0.9923
17.50	0.0080	17.4038	0.5032
18.00	-0.0017	17.9184	0.2902
19.00	-0.0056	18.9304	0.1141
20.00	-0.0061	19.9374	0.0455
22.00	-0.0058	21.9476	0.0011
25.00	-0.0051	24.9587	0.0080
28.00	-0.0044	27.9667	0.0059
30.00	-0.0040	29.9709	0.0045
35.00	-0.0031	34.9785	0.0018
50.00	-0.0017	49.9895	0.0000

FIG. 3. Adiabatic dipole moments of the $X^1\Sigma^+$ and $B^1\Sigma^+$ states (top) and $B^1\Sigma^+ \leftarrow X^1\Sigma^+$ dipole transition moment (bottom) of LiCl. (Solid curve, two-state averaged MRSDCI calculation; dashed curve, semiempirical valence-bond calculations of Zeiri and Balint-Kurti (Ref. 15).

below the crossing point energy, thus reproducing the ionic character of the $X^1\Sigma^+$ for internuclear separations shorter than the avoided crossing. The function $\mu(v)$ reaches its maximum, 29.65 D, for $v = 139$, a vibrational level energetically close to the crossing point. For higher vibrational levels, corresponding to internuclear distances beyond the crossing, $\mu(v)$ tends to zero in a similar way as the dipole moment function of the adiabatic $X^1\Sigma^+$ state. For a given v'' , the vibrational matrix elements of the dipole moment decrease rapidly as Δv increases, consistent with the usual observations that the fundamental ($\Delta v = 1$) transition is stronger than the first overtone ($\Delta v = 2$) transition, which in turn is stronger than the second overtone ($\Delta v = 3$) transition.

IV. CONCLUSION

Single- and double-excitation configuration interaction wave functions constructed from MCSCF/SA molecular orbitals provide a globally accurate adiabatic representation of the $X^1\Sigma^+$ and $B^1\Sigma^+$ electronic states of LiCl. The potential energy curves are continuously described in the avoided crossing region, with a precision unmatched by previous semiempirical valence-bond calculations. In addition, our MRSDCI energies for the $B^1\Sigma^+$ state significantly improve on the valence-bond results at short range. The spectroscopic

TABLE V. Vibrational matrix elements of the $X^1\Sigma^+$ state dipole moment of $^7\text{Li}^{35}\text{Cl}$ (in debye).^a

v''/v'	0	1	2	3	4	5
0	7.321	2.87(-1)	-1.5(-2)	1(-3)	—	—
1		7.404	4.08(-1)	-2.6(-2)	3(-3)	—
2			7.487	5.02(-1)	-3.7(-2)	5(-3)
3				7.572	5.84(-1)	-4.8(-2)
4					7.657	6.56(-1)
5						7.7434

^aVibrational matrix elements are calculated in this work with rotational quantum numbers $J''=0$ and $J'=1$ [$R(0)$ line] for $X^1\Sigma^+ \leftarrow X^1\Sigma^+$ transitions. Notation, $x(-n) \equiv x \times 10^{-n}$. A single dash means less than 0.001. Only transitions with $v' \geq v''$ are considered to avoid redundancy.

constants and vibrational energy levels derived for the $X^1\Sigma^+$ state are found to be in excellent agreement with experimental values. The vibrationally averaged dipole moment of the *ab initio* $X^1\Sigma^+$ state reproduces the spectroscopic values to within 3%.

The *ab initio* results of the present work should provide accurate photodissociation cross sections and absorption oscillator strengths for LiCl, which are of interest in astrophysics. In particular, in cool brown dwarf atmospheres, where lithium chloride appears to be the dominant Li-bearing gas for a large range of temperatures and pressures,⁴¹ LiCl may be a significant source of line and continuum opacity over a range of wavelengths from the infrared to the near ultraviolet. Calculations of the opacity resulting from LiCl in cool atmospheres are underway.

ACKNOWLEDGMENTS

This work was supported by NASA Grant No. NAG5-10551, and partially supported by the National Science Foundation through a grant to the Institute for Theoretical Atomic, Molecular and Optical Physics at Harvard University and Smithsonian Astrophysical Observatory. P.F.W. acknowledges ITAMP at Harvard University and SAO for travel support. The authors are grateful to A. Dalgarno and H. Sadeghpour for helpful discussions about this work, and to P. H. Hauschildt and A. Schweitzer for indicating to us the importance of LiCl and for providing computer resources.

- ¹L. Pauling, *Nature of the Chemical Bond*, 3rd ed. (Cornell University Press, Ithaca, New York, 1960).
- ²L. D. Landau, *Phys. Z. Sowjetunion* **2**, 46 (1932).
- ³C. Zener, *Proc. R. Soc. London, Ser. A* **137**, 696 (1932).
- ⁴C. J. Bardeen, J. Che, K. R. Wilson, V. V. Yakovlev, P. Cong, B. Kohler, J. L. Krause, and M. Messina, *J. Phys. Chem. A* **101**, 3815 (1997).
- ⁵H. Tang and S. A. Rice, *J. Phys. Chem. A* **101**, 9587 (1997).
- ⁶M. Grønager and N. E. Henriksen, *J. Chem. Phys.* **109**, 4335 (1998).
- ⁷M. Shapiro and P. Brumer, *Principles of the Quantum Control of Molecular Processes* (Wiley, Hoboken, NJ, 2003).
- ⁸A. Honig, M. Mandel, M. L. Stitch, and C. H. Townes, *Phys. Rev.* **96**, 629 (1954).
- ⁹D. R. Lide, P. Cahill, and L. P. Gold, *J. Chem. Phys.* **40**, 156 (1964).
- ¹⁰T. L. Story, Ph. D. dissertation, University of California, Lawrence Radiation Laboratory, Berkeley, 1968.
- ¹¹K. P. Huber and G. Herzberg, *Molecular Spectra and Molecular Structure*,

- Vol. IV, Constants of Diatomic Molecules* (Van Nostrand Reinhold, New York, 1979).
- ¹²H. Jones and J. Lindenmayer, *Chem. Phys. Lett.* **135**, 189 (1987).
 - ¹³F. Ito, P. Klose, T. Nakanaga, H. Takeo, and H. Jones, *J. Mol. Spectrosc.* **194**, 17 (1999).
 - ¹⁴G. A. Thompson, A. G. Maki, W. B. Olson, and A. Weber, *J. Mol. Spectrosc.* **124**, 130 (1987).
 - ¹⁵Y. Zeiri and G. G. Balint-Kurti, *J. Mol. Spectrosc.* **99**, 1 (1983).
 - ¹⁶J. F. Ogilvie, *Spectrosc. Lett.* **25**, 1341 (1992).
 - ¹⁷D. L. Cooper, S. Bienstock, and A. Dalgarno, *J. Chem. Phys.* **86**, 3845 (1987).
 - ¹⁸M. Seth, M. Pernpointner, G. A. Bowmaker, and P. Schwerdtfeger, *Mol. Phys.* **96**, 1767 (1999).
 - ¹⁹C. Sousa, D. Dominguez-Ariza, C. de Graaf, and F. Illas, *J. Chem. Phys.* **113**, 9940 (2000).
 - ²⁰T. C. Melville and A. Coxon, *Spectrochim. Acta, Part A* **57**, 1171 (2001).
 - ²¹T. Pluta, *Mol. Phys.* **99**, 1535 (2001).
 - ²²R. J. Buenker and S. D. Peyerimhoff, *Chem. Phys. Lett.* **34**, 225 (1975).
 - ²³H.-J. Werner and W. Meyer, *J. Chem. Phys.* **74**, 5802 (1981).
 - ²⁴J. Finley, P.-A. Malmqvist, B. O. Roos, and L. Serrano-Andrés, *Chem. Phys. Lett.* **288**, 299 (1998).
 - ²⁵C. W. Bauschlicher, Jr. and S. R. Langhoff, *J. Chem. Phys.* **89**, 4246 (1988).
 - ²⁶C. E. Moore, *Atomic Energy Levels*, NBS Reference Data System No. 34 (US GPO, Washington DC, 1971).
 - ²⁷R. D. Mead, A. E. Stevens, and W. C. Lineberger, in *Gas Phase Ion Chemistry*, edited by M. T. Bowers (Academic, Orlando, 1984), Vol. 3, p. 213.
 - ²⁸A. D. Pradhan, K. P. Kirby, and A. Dalgarno, *J. Chem. Phys.* **95**, 9009 (1991).
 - ²⁹A. Dalgarno, K. Kirby, and P. C. Stancil, *Astrophys. J.* **458**, 397 (1996).
 - ³⁰A. D. McLean, M. Yoshimine, B. H. Lengsfeld, P. S. Bagus, and B. Liu, in *MOTECC 91*, edited by E. Clementi (Elsevier, Leiden, 1991).
 - ³¹P. Brumer and M. Karplus, *J. Chem. Phys.* **58**, 3903 (1973).
 - ³²Y. Zeiri and M. Shapiro, *J. Chem. Phys.* **31**, 217 (1978).
 - ³³A. B. Alekseyev, H.-P. Liebermann, R. J. Buenker, N. Balakrishnan, H. R. Sadeghpour, S. T. Cornett, and M. J. Cavagnero, *J. Chem. Phys.* **113**, 1514 (2000).
 - ³⁴NIST Atomic Spectra Database (1999), http://aeldata.phy.nist.gov/cgi-bin/AtData/main_asd
 - ³⁵J. W. Cooley, *Math. Comput.* **15**, 363 (1961).
 - ³⁶In atomic mass units, Aston's scale.
 - ³⁷L. Brewer and E. Brackett, *Chem. Rev.* **61**, 425 (1961).
 - ³⁸E. M. Bulewicz, L. F. Phillips, and T. M. Sugden, *Trans. Faraday Soc.* **57**, 921 (1961).
 - ³⁹G. Herzberg, *Molecular Spectra and Molecular Structure, Vol. I, Spectra of Diatomic Molecules* (Van Nostrand Reinhold, New York, 1950).
 - ⁴⁰A. J. Hebert, F. J. Lovas, C. A. Melendres, C. D. Hollowell, T. L. Story, Jr., and K. Street, Jr., *J. Chem. Phys.* **48**, 2824 (1968).
 - ⁴¹K. Ladders, *Astrophys. J.* **519**, 793 (1999).